Growth and form of melanoma cell colonies

Growth and form of melanoma cell colonies

Massimiliano Maria Baraldi[1], **Alexander A Alemi**[2], **James P Sethna**[2], **Sergio Caracciolo**[1,3], **Caterina A M La Porta**[4] **and Stefano Zapperi**[5,6]

[1] Physics Department, University of Milano, via Celoria 16, I-20133 Milano, Italy
[2] LASSP, Department of Physics, Clark Hall, Cornell University, Ithaca, NY 14853-2501, USA
[3] INFN, via Celoria 16, I-20133 Milano, Italy
[4] Department of Biosciences, University of Milano, via Celoria 26, I-20133 Milano, Italy
[5] CNR-IENI, Via R Cozzi 53, I-20125 Milano, Italy
[6] ISI Foundation, Via Alassio 11/C, 10126 Torino, Italy
E-mail: massimilianomaria.baraldi@studenti.unimi.it, aaa244@cornell.edu, sethna@lassp.cornell.edu, sergio.caracciolo@mi.infn.it, caterina.laporta@unimi.it and stefano.zapperi@cnr.it

Abstract. We study the statistical properties of melanoma cell colonies grown *in vitro* by analyzing the results of crystal violet assays at different concentrations of initial plated cells and for different growth times. The distribution of colony sizes is described well by a continuous time branching process. To characterize the shape fluctuations of the colonies, we compute the distribution of eccentricities. The experimental results are compared with numerical results for models of random division of elastic cells, showing that experimental results are best reproduced by restricting cell division to the outer rim of the colony. Our results serve to illustrate the wealth of information that can be extracted by a standard experimental method such as the crystal violet assay.

Contents

1. Introduction

Understanding how tumors grow is a long-standing problem whose complexity stems from the interplay of several factors, including cancer cell heterogeneity, interactions with the environment and stochastic mutations during progression. Some interesting features of tumor growth can, however, be inferred from *in vitro* experiments where cancer cell duplication and spreading can be observed in ideal conditions. In particular, colony formation assays have a practical interest in drug testing, where one compares cell colonies formed with or without a drug. Due to its relative simplicity, cancer colony formation has attracted the interest of statistical physicists [1]–[5], who mostly focused on the morphological properties of individual colonies—e.g. the colony boundary, which is well described by self-affine scaling [2]–[5]. Colony formation also represents the ideal playground to test mathematical models for tumor growth based on individual cell mechanics [6]–[9] , cellular automata [10, 11] or differential equations [12].

In typical cancer cell colony growth experiments, such as in the crystal violet assay, biologists study the distribution of colonies formed in multiwells. In this case, one is usually interested just in the number of colony forming clones. The experiments, however, provide a wealth of other useful information concerning the distributions of colony sizes and shapes that are rarely analyzed in detail. In this paper, we illustrate this point by studying the statistical properties of colonies formed by melanoma cells *in vitro* for different growth times. In particular, we consider the distribution of sizes and shapes. By using automatic image analysis methods, we are able to study with relative ease thousands of colonies

formed of hundreds of cells. As a comparison, earlier studies based on manual counting of the cells in the colonies could perform statistics over around 50 colonies [1]. Here we show that the experimentally measured colony size distributions are quantitatively described by a branching process [13, 14], a class of models that has been used extensively in the past to model the growth of stem cells [15]–[20] and cancer cells [1], [21]–[25].

The main limitation of branching processes is due to their mean-field nature, which does not take into account the geometry of the cellular arrangement inside a tumor. Hence to understand the distribution of colony shapes, quantified by their eccentricity, we use individual cell models in which cells interact either by elastic interactions [6, 7] or by simple geometrical hindrance, corresponding in the simplest example to the Eden growth model [26]. We find that the Eden model describes the experimental eccentricity data more accurately than the elastic interaction model. Our results show that a comparison between experimental and theoretical results provides useful indications for building realistic models for cancer growth.

The paper is organized as follows: in section 2 we discuss the experiments and the data analysis, in sections 3 and 4 we report and discuss size and shape distributions, respectively, and section 5 is devoted to conclusions.

## 2. Cancer cell colony formation: experiments and data analysis

2.1. Colony growth

To study the formation of melanoma cell colonies *in vitro*, we use human IGR39 cells, obtained from Deutsche Sammlung von Mikroorganismen und Zellkulturen GmbH and cultured as previously described [27]. IGR39 cells are derived from a primary amelanotic cutaneous tumor. Cells are plated on 6-well plates and stained after 8 days or 10 days. Next, cells are fixed with 3.7% paraformaldeide (PFA) for 5 min and then stained for 30 min with 0.05% crystal violet solution. After twice washing with tap water, the plates are drained by inversion for a couple of minutes. In order to control the merging of different colonies, the experiments are performed with different initial cell concentrations N_0. In particular, we use $N_0 = 1, 10, 20, 30, 80, 100, 150, 250$ cells/well for cells growing 8 days, and $N_0 = 1, 10, 50, 100, 150$ for cells growing 10 days.

2.2. Image analysis

We acquired images of the six wells by a simple scanner with a resolution of 600×2400 dpi. The color images are then transformed into black and white (see figure 1). In order to do this automatically, avoiding errors associated with shadows and noise, we separate the colonies from the background using an edge detection difference with the Gaussian algorithm [28]. In this way, even small colonies can be identified from the background and the transformation into a black and white image is insensitive to the threshold used. Some of the wells have to be discarded, either because a considerable fraction of the cells detached or because the staining was too noisy to process. In addition, we avoid errors associated with the boundary of the well by considering only colonies inside an inner circle of radius $R = 650$ px, while the well had a radius of 800 px.

Next we perform a cluster analysis to isolate individual colonies. This is done in two steps: we first perform an Hoshen–Kopelman algorithm [29] to identify clusters that are

3
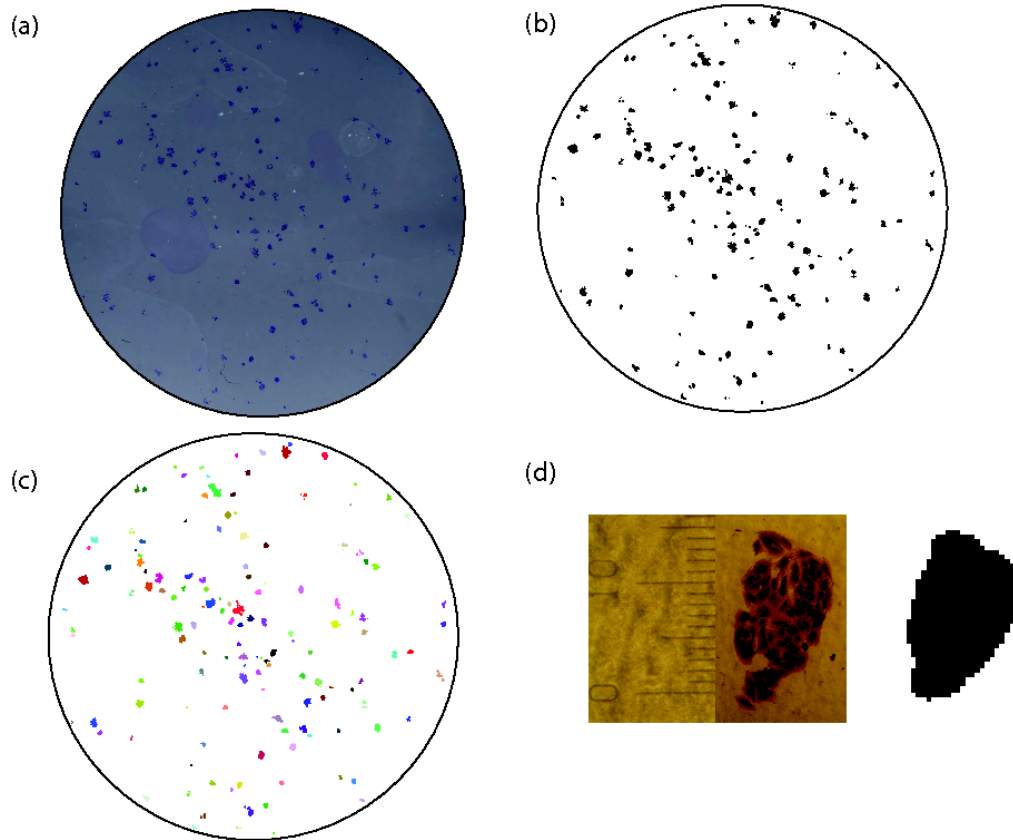
Figure 1. An illustration of the cluster algorithm. (a) Melanoma cell colonies formed after 8 days in a single well. (b) The picture is transformed into a black & white image. (c) Individual colonies, identified using the cluster algorithm, are colored here with random colors for visualization purposes. (d) A digitized cluster can be compared with an image of the same cluster obtained with a microscope in order to quantify the cell density versus area.

separated by at least one pixel. This results sometimes in very small clusters surrounding large ones. We think that this is due to the fact that individual cells can sometime separate from the boundary of the colony during the division process. We therefore devise an algorithm to join small clusters to large ones. We first divide small and large clusters depending on a threshold S^* that we set equal to 100 px. We then scan the lattice, and if a small cluster is within a radius $r = 8$ px from a large cluster, we join them together into a single cluster. We test the effect of the value of S^* on the final colony size distribution and find only small variations in the final outcome. Finally, we convert the cluster size from pixels to cells using a microscope endowed with a resolution of 1 μm. We count the number of cells contained in a set of colonies, from which we estimate a conversion factor $p = 0.14 \pm 0.05$ cells/px, or equivalently a cell corresponds to seven to eight px.

2.3. Cluster arrangement

According to the experimental protocol, cells are initially spread randomly and uniformly on the wells. We check if this assumption is correct by comparing the spatial arrangement
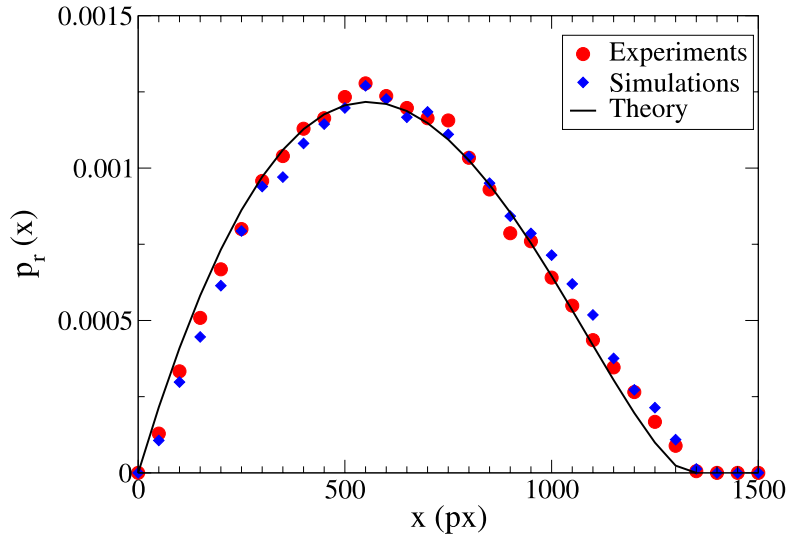
Figure 2. The distribution of the distances between the colonies' centers of mass compared with analytical and numerical predictions from a random Poisson process.

of the colonies to a random process. This is achieved by comparing the distribution of the (Euclidean) distances between the center of mass of the colonies with the distribution $p_r(x) = p_r(x_{i,j} = x)$ of distances $x_{i,j} = \|\mathbf{x_i} - \mathbf{x_j}\|$ obtained from a Poisson process in a circle of radius r. Figure 2 shows the experimental distribution of $p_r(x)$ and the simulated distribution compared with the analytical expression given by

$$p_r(x) = \frac{2x}{r^2}\left(\frac{2}{\pi}\arccos\left(\frac{x}{2r}\right) - \frac{x}{\pi r}\sqrt{1 - \frac{x^2}{4r^2}}\right). \tag{1}$$

We also report the result of a numerical distribution obtained by throwing random points in a circular well. The good agreement between experimental data and analytical curves shows that colonies are randomly distributed in the well, without noticeable interactions between them. In principle, cell motility could affect the final position of the colony. Time lapse microscopy shows, however, that in the present experimental conditions cells move very little as compared with the typical distance between the colonies.

2.4. Density dependence

Experiments are performed at different initial densities N_0 in order to test the dependence of the resulting colonies on the initial condition. In figure 3(a) we plot the number of colonies as a function of N_0. As expected, the number of colonies N_c is roughly equal to the number of cells plated initially, providing a test of the validity of the cluster algorithm. Next, in the inset of figure 3(a), we report the average colony size $\langle s \rangle$ as a function of N_0. These show a small dependence, especially for colonies grown for 8 days. This result provides indirect evidence that the merging of different colonies is a marginal effect. We expect that using a larger initial density would make the results less reliable. In figure 3
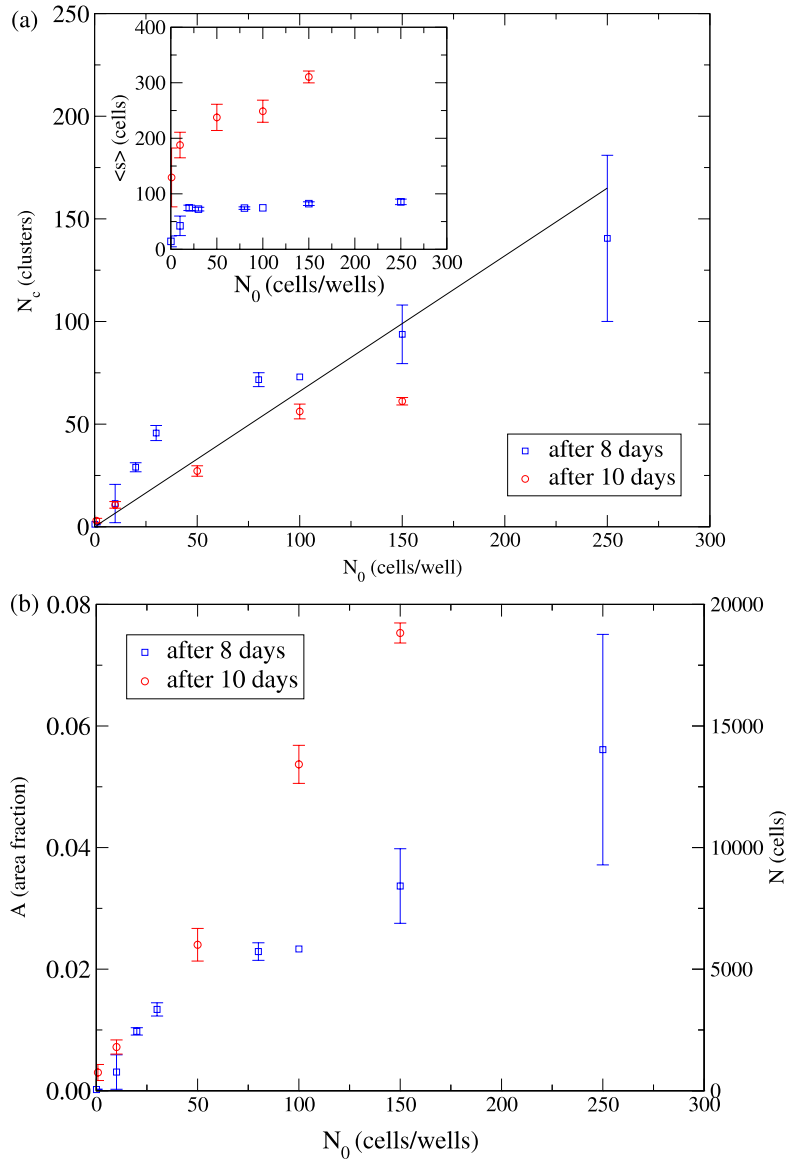
Figure 3. The role of the initial cell density in cluster statistics. (a) The total number of colonies grows linearly with the number of the initial cells N_0 present in each well but is almost independent of the incubation time. The slope of the line is the ratio of the area analyzed to the total area of the well. The inset shows that the average colony size is reasonably constant as the initial density is varied. (b) The fraction of area covered A and the total number of cells N grow linearly with the initial number of cells, where the slope depends on the incubation time. Error bars are the standard errors obtained by considering data from different wells (typically six or fewer wells are considered).

we report the fraction of total area A that is covered by cells in each well as a function of the initial cell density N_0. Figure 3 also reports the total number of cells N in each well obtained by counting the number of occupied pixels and then dividing by the conversion factor $p = 0.14$ cells/px. As expected, both A and N grow linearly with N_0.
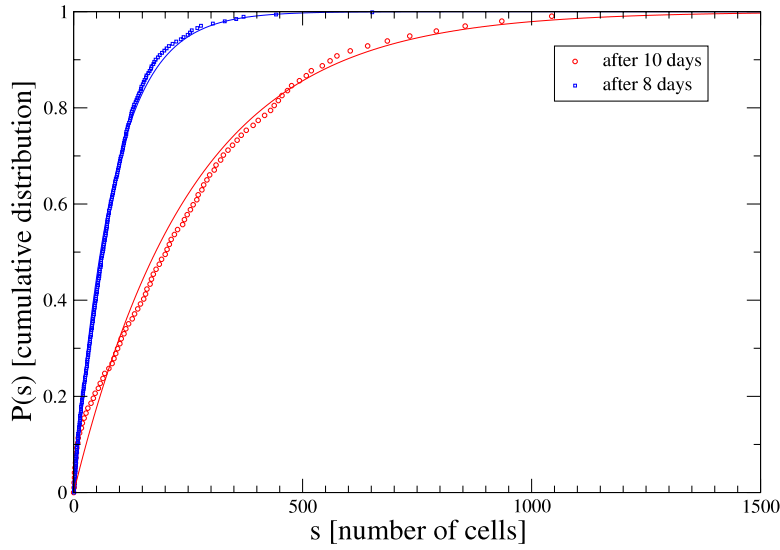
Figure 4. The distribution of colony sizes after 8 and 10 days of growth. The distribution is obtained by collecting all the colonies obtained for all the different values of N_0, corresponding to 32 and 30 wells, 2347 and 1067 colonies of average size $\langle S \rangle \simeq 85$ and $\langle S \rangle \simeq 258$ for 8 and 10 days respectively. The curves represent the simulation of the continuum time branching process using the parameters obtained from the maximum likelihood estimate.

3. Colony size distributions

In order to describe the fluctuations in the growth of melanoma cell colonies, we compute the cumulative distribution of colony sizes grown for 8 or 10 days, collecting together data obtained in different wells and for different values of N_0. The cumulative distribution $P(s)$ is related to the probability density function $p(s)$ by

$$P(s) = \sum_{s'=1}^{s} p(s'). \tag{2}$$

As shown in figure 4, colonies become larger as time passes and consequently the cumulative distribution shifts to the right.

To understand more quantitatively the experimentally measured colony size distribution, we consider a simple continuous time branching process in which each cell duplicates at rate γ and dies at rate β. Here we are interested in the evolution of the size distribution of colony sizes $p(s,t)$, defined as the probability to find a colony of size s at time t, where time is measured in days. The probability density function evolves according to the following master equation

$$\frac{\mathrm{d}p(s,t)}{\mathrm{d}t} = \gamma(s-1)\,p(s-1,t) + \beta(s+1)\,p(s+1,t) - (\gamma+\beta)s\,p(s,t), \tag{3}$$

starting with an initial condition $p(s,0) = \delta_{s,1}$. From equation (3), we can obtain an equation for the first moment, the average colony size $\langle s \rangle$,

$$\frac{\mathrm{d}\langle s \rangle}{\mathrm{d}t} = (\gamma - \beta)\langle s \rangle, \tag{4}$$

yielding an exponential growth

$$\langle s(t) \rangle = \exp[(\gamma - \beta)t]. \tag{5}$$

The model described by equation (3) is a particular case of the *birth and death process* and its explicit solution is given by (see [13] page 104):

$$p(0,t) = 1 - \frac{\langle s(t) \rangle (\gamma - \beta)}{\gamma \langle s(t) \rangle - \beta} \tag{6}$$

$$p(s,t) = \langle s(t) \rangle \left(\frac{\gamma - \beta}{\gamma \langle s(t) \rangle - \beta} \right)^2 \left(1 - \frac{\gamma - \beta}{\gamma \langle s(t) \rangle - \beta} \right)^{s-1} \qquad \text{for } s \geq 1. \tag{7}$$

To obtain a quantitative comparison between theory and experiments, we employ the maximum likelihood method and estimate the best values for γ and β, with the constraints $\beta \geq 0$ and $\gamma \geq 0$. In practice, using an iterative optimization scheme we find the values of γ and β that maximize the cost function given by

$$\mathcal{L} = \sum_i \log(p(s_i^{(t=8)}, 8)) + \sum_j \log p(s_j^{(t=10)}, 10) \tag{8}$$

where $s_i^{(t=8)}$ and $s_j^{(t=10)}$ are the experimentally measured colony sizes after 8 and 10 days, respectively. Using this scheme, the best fit yields $\gamma = 0.55$ divisions day^{-1} and sets β to its limiting value of zero. In the limit $\beta \to 0$, the model is equivalent to the Yule problem [13] and the solution is given in simpler form by [13]

$$p(s,t) = \mathrm{e}^{-\gamma t}(1 - \mathrm{e}^{-\gamma t})^{s-1} \qquad \text{for } s \geq 1. \tag{9}$$

The fitted value for γ can be compared with previous experiments on melanoma growth, but at much higher cell density, which yielded $\gamma \simeq 0.4$ divisions day^{-1} [25]. This is compatible with the general idea that the growth rate decreases when the cell density is higher.

4. Colony shapes

4.1. Eccentricities

Cancer cell colonies come in different sizes but also in different shapes. A natural measure of the shape of a colony is the inertia moment tensor, which we define with respect to the center of mass of each colony when each pixel is assigned unit mass. The principal moments of inertia λ_M and λ_m, where M denote the maximum and m denote the minimum eigenvalue, and the corresponding principal axes found by diagonalizing the inertia moment tensor. Here we characterize the shape of each cluster with the eccentricity defined as

$$\epsilon \equiv \sqrt{1 - \left(\frac{\lambda_m}{\lambda_M} \right)^2}. \tag{10}$$

In figure 5 we report the cumulative distribution of eccentricities $P(\epsilon)$ for colonies grown 8 or 10 days. The figure shows that the distribution shifts to the left with time, suggesting that the colonies become more isotropic as they grow. In percolation clusters, the ratio λ_M/λ_m is found to display universal corrections to scaling [30]. Similar relations have
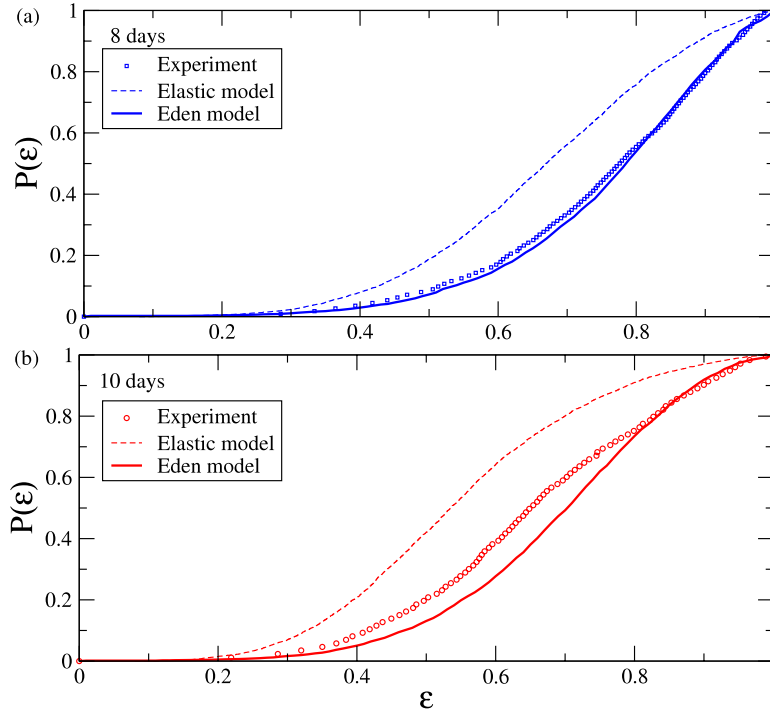
Figure 5. The distribution of eccentricities for colonies grown for (a) 8 days and (b) 10 days. The dashed line is the result of the cell mechanics model, the solid line is the result of the Eden model. In both cases, the models have been simulated with the parameters obtained from the fit of the colony size distribution with the continuum time branching process.

been obtained in other models, such as polymers [31] and lattice animals [32]. It would be interesting to compute directly the correction to the scaling exponent for our clusters in analogy with [30], but our data appear to be insufficient for this purpose.

4.2. Modeling shape fluctuations: elastic cell model

The continuous time branching process used to describe the colony size distribution does not consider geometry and does not provide any information on the shape of the colony. To overcome this limitation, we consider a model of elastic spherical cells dividing randomly in two dimensions. The cells interact with a simple Hertz pair potential [6]

$$V(r_{ij}) = \frac{4E(2R - r_{ij})}{15(1 - \nu^2)}\sqrt{\frac{R}{2}}, \qquad \text{for } r_{ij} < 2R \tag{11}$$

where R is the cell radius, r_{ij} is the distance between the cell centers, E is the Young modulus and ν is the Poisson ratio. Cell division occurs randomly at rate γ. To this end we use the Gillespie algorithm [33]: we randomly select a cell and perform a cell division at time sequences where the step at time t is chosen according to a Poisson distribution with rate $s\gamma$, where s is the number of cells in the colony at time t. Choosing $\gamma = 0.55$ divisions day^{-1}, we reproduce the experimentally measured size distribution. Cell division is simulated by replacing the dividing cell by two randomly oriented new

cells placed at distance $r = R/10$. The system is then relaxed to mechanical equilibrium, locally minimizing the total elastic energy

$$E_{\text{el}} = \sum_{\langle ij \rangle} V(r_{ij}), \tag{12}$$

where the sum is restricted to cells in contact.

Using this model we simulate a set of 4000 colonies after 8 and 10 days of growth. The resulting cumulative distribution of eccentricities is reported in figure 5. We can see systematic differences with respect to the experimental data.

4.3. Modeling shape fluctuations: Eden model

A possible explanation for this result is that cell division does not occur homogeneously throughout the colony as we assume in the model. Experimental results for other tumors show that cell division is mostly confined to the outer rim of the colony, with little division occurring in the bulk [2]. We note that perimeter growth is somewhat incompatible with our branching process analysis of the size distribution, since asymptotically the growth of the colony would not be exponential. For the short times and small cluster sizes analyzed here, however, growth is indeed exponential, as shown by experiments [2] and models [9], so that a mean-field analysis based on branching processes yields reliable results.

To take into account the fact that the rate of division depends on the cell location we have to go beyond a mean-field description. The simplest growth model to describe a colony in which cell division is restricted to the periphery is the Eden model [26], originally devised to describe bacterial colonies, but recently shown to reproduce the roughness of cancer cell colonies [5]. The Eden model can be simulated on a lattice as in the original paper [26] by randomly growing sites whose nearest neighbors are already occupied. In this form, however, Eden clusters inherit the anisotropy of the square lattice [34]. This problem is overcome in the off-lattice version of the model, in which circular particles are added randomly to the aggregate taking care to avoid any overlap between the particles [35]–[37]. Lattice anisotropy can be avoided even in the square lattice by using appropriate growth rules, as shown in [38]. Here we use the latter approach to grow Eden clusters.

We consider a two-dimensional square lattice and start with an initial seed. At each step we select an occupied site in the lattice with at least one empty nearest neighbor site. We randomly select one of the empty sites j and occupy it with a probability p depending on n_j the number of occupied nearest neighbors of the site j as $p = n_j/4$. This particular version of the Eden model has been shown to result in clusters that are asymptotically circular, thus reducing lattice anisotropy [38]. We use this model to generate a set of clusters with size distributions similar to the experimental ones. This is done in practice by implementing the same Gillespie algorithm employed for the elastic cell model. We next compute the distribution of eccentricities after 8 and 10 days. The results, shown in figure 5, are in good agreement with experimental data.

5. Discussion

In this paper we have performed a statistical analysis of the growth of melanoma cell colonies using the crystal violet assay, a standard method in cancer biology. While most

(but not all [1]) previous studies of cancer colony formation focused on the morphology of a single colony [2]–[5], we consider the time evolution of the distribution of sizes and shapes of different colonies. The colony size distribution is quantitatively described by a birth and death process, with a negligible rate of cell death. We next analyze the fluctuations of colony shapes as described by the eccentricity distribution obtained from the eigenvalues of the moment of inertia tensor. We compare the experimentally measured distributions with two simple models of cell proliferation: a mechanical model in which cells duplicate and interact elastically and a geometrical model in which cells duplicate only if the surrounding space is empty. The latter case corresponds to the Eden model [26], which we simulate using a lattice version that minimizes systematic lattice anisotropies [38].

Our results indicate that the Eden model does a better job at reproducing the experiments than the elastic particle model, indicating that cell division is hindered just by geometrical constraints, since there is no difference in terms of nutrients or oxygen between the interior and the boundary of the colonies here. This is confirmed by experimental results showing that duplication is reduced in the interior of the colony [2]. A purely elastic model, such as the one we employ here, is not adequate to describe the data, but one could introduce geometrical constraints in this type of model by reducing the duplication rate for cells under compression [9].

We notice that the boundary surface of the Eden model clusters is self-affine, with a roughness exponent described by the Kardar–Parisi–Zhang (KPZ) equation [39]. Other experiments on individual colony growth indicate that the scaling behavior of the surface falls into the KPZ universality class [4, 5]. Earlier results suggesting a different universality class [2] have been attributed to artifacts in the statistical analysis [3, 40]. Our colonies are too small to measure the roughness exponent directly, but it is still interesting to note that the Eden model describes their shapes. In conclusion, our results provide an illustration of the wealth of quantitative information that can be extracted by a standard biological method such as the crystal violet assay.

Acknowledgments

References

[1] Kimmel M and Axelrod D E, 1991 *J. Theor. Biol.* **153** 157–80
[2] Bru A, Albertos S, Subiza J L, Garcia-Asenjio J L and Bru I, 2003 *Biophys. J.* **85** 2948–61
[3] Buceta J and Galeano J, 2005 *Biophys. J.* **88** 3734–6
[4] Huergo M A C, Pasquale M A, González P H, Bolzán A E and Arvia A J, 2011 *Phys. Rev. E* **84** 021917
[5] Huergo M A C, Pasquale M A, González P H, Bolzán A E and Arvia A J, 2012 *Phys. Rev. E* **85** 011918
[6] Drasdo D, Kree R and McCaskill J, 1995 *Phys. Rev. E* **52** 6635–57
[7] Galle J, Loeffler M and Drasdo D, 2005 *Biophys. J.* **88** 62–75
[8] Galle J, Hoffmann M and Aust G, 2009 *J. Math. Biol.* **58** 261–83
[9] Drasdo D and Hoehme S, 2012 *New J. Phys.* **14** 055025
[10] Loeffler M, Potten C and Wichmann H, 1987 *Virchows Arch. Abteilung B Cell Pathol.* **53** 286–300
[11] Block M, Schoell E and Drasdo D, 2007 *Phys. Rev. Lett.* **99** 248101
[12] Chatelain C, Balois T, Ciarletta P and Amar M B, 2011 *New J. Phys.* **13** 115013
[13] Harris T E, 1989 *The Theory of Branching Processes* (New York: Dover)

[14] Kimmel M and Axelrod D E, 2002 *Branching Processes in Biology* (New York: Springer)
[15] Vogel H, Niewisch H and Matioli G, 1968 *J. Cell Physiol.* **72** 221–8
[16] Matioli G, Niewisch H and Vogel H, 1970 *Rev. Eur. Etud. Clin. Biol.* **15** 20–2
[17] Potten C S and Morris R J, 1988 *J. Cell Sci. Suppl.* **10** 45–62
[18] Clayton E, Doup D P, Klein A M, Winton D J, Simons B D and Jones P H, 2007 *Nature* **446** 185–9
[19] Antal T and Krapivsky P L, 2010 *J. Stat. Mech.* P07028
[20] Itzkovitz S, Blat I C, Jacks T, Clevers H and van Oudenaarden A, 2012 *Cell* **148** 608–19
[21] Michor F, Hughes T P, Iwasa Y, Branford S, Shah N P, Sawyers C L and Nowak M A, 2005 *Nature* **435** 1267–70
[22] Ashkenazi R, Gentry S N and Jackson T L, 2008 *Neoplasia* **10** 1170–82
[23] Michor F, 2008 *J. Clin. Oncol.* **26** 2854–61
[24] Tomasetti C and Levy D, 2010 *Proc. Nat. Acad. Sci.* A **107** 16766–71
[25] La Porta C A M, Zapperi S and Sethna J P, 2012 *PLoS Comput. Biol.* **8** e1002316
[26] Eden M, 1961 *Proc. 4th Berkeley Symposium on Mathematical Statistics and Probability* vol IV, ed F Neyman (Berkeley: University of California Press) p 233
[27] Taghizadeh R, Noh M, Huh Y H, Ciusani E, Sigalotti L, Maio M, Arosio B, Nicotra M R, Natali P, Sherley J L and La Porta C A M, 2010 *PLoS One* **5** e15183
[28] Marr D and Hildreth E, 1980 *Proc. R. Soc.* B **207** 187–217
[29] Hoshen J and Kopelman R, 1976 *Phys. Rev.* B **14** 3438–45
[30] Family F, Vicsek T and Meakin P, 1985 *Phys. Rev. Lett.* **55** 641–4
[31] Aronovitz J A and Nelson D R, 1986 *J. Physique* **47** 1445–56
[32] Aronovitz J A and Stephen M J, 1987 *J. Phys. A: Math. Gen.* **20** 2539
[33] Gillespie D T, 1976 *J. Comput. Phys.* **22** 403–34
[34] Freche P, Stauffer D and Stanley H E, 1985 *J. Phys. A: Math. Gen.* **18** L1163
[35] Wang C Y, Liu P L and Bassingthwaighte J B, 1995 *J. Phys. A: Math. Gen.* **28** 2141
[36] Ferreira S C and Alves S G, 2006 *J. Stat. Mech.* P11007
[37] Alves S G, Oliveira T J and Ferreira S C, 2011 *Europhys. Lett.* **96** 48003
[38] Paiva L R and Ferreira S C, 2007 *J. Phys. A: Math. Theor.* **40** F43
[39] Kardar M, Parisi G and Zhang Y C, 1986 *Phys. Rev. Lett.* **56** 889–92
[40] Pastor J and Galeano J, 2007 *Central Eur. J. Phys.* **5** 539–48